

Supplementary material

SM1 - Storm surge analysis

The storm-surge scenarios have been derived applying the classical approach of maritime analysis taking into account the main components of wave climate assessment, wave transformation up to wave breaking to estimate wave conditions during the wave travel and ends to the assessment of the wave setup and runup on beach for each transect.

The maritime wave climate assessment and storm surge data for the study areas have been evaluated through the Forecast/hindcast system for the Mediterranean Sea developed by the Department of Environmental, Chemistry and Civil Engineering of University of Genoa (Mentaschi et al., 2013, 2015). Wave climate assessment originates from a re-analysis of atmospheric and wave conditions, producing an hindcast database spanning from January 1979 till the end of December 2016 over the domain employed for the atmospheric and wave condition simulations.

The hindcast dataset for wave characteristics can be employed for Coastal and Ocean

The system is mainly based on the WAVEWATCH III (WWIII) model in the Mediterranean. This model allows the climate wave analysis referring to several case studies related to heavy storms observed in this basin in the last twenty-five years. Wherever available, the simulation results have been validated using buoy data provided by different official sources.

Wind forcing has been simulated using the WRF (Weather and Research Forecasting) model for all the case studies, while the wave simulations are carried out using the WWIII model. The simulated and observed data are compared through statistical error measures like Normalized Bias (NBI), Normalized Root Mean Square Error (NMRSE), also known as Scatter Index, and Correlation Coefficient (CORR). Since model performances are not uniform in space and time, all the statistical error measures have been evaluated taking into account different groups of buoys chosen depending on the geographical location in the Mediterranean basin or on the sea conditions (stormy or not stormy).

For the investigated site, the significant wave height polar histogram and the 2-D histogram for significant wave height, H_s , and peak period, T_p , are evaluated to derive the local wave climate scenarios, as well as the Extreme Value Analysis (EVA) for the H_s , is provided too. The extreme value analysis for all the available data has been carried out following the Peak Over Threshold (POT); taking into account all peak storm event values exceeding a 0.98 percentile imposing a minimum inter-arrival time between two storms of 12 hours.

By the use of wave climate data referring to ordinary and extreme storm wave conditions, in terms of return period (RT), respectively $RT=1$ year and $RT=100$ years, wave setup and wave run-up were estimated. In the analysis wind set up was neglected. We used the topo-bathymetric information collected for each transects considered.

In detail, using the equivalent Snell's law, the wave height at a location i is related to the wave height in deep water H_0 by

$$H_i = H_0 K_S K_R$$

Where K_S is the shoaling coefficient and K_R is the refraction coefficient caused by the shape of bottom topography which influences the direction of wave travel. When the wave motion interacts with the bottom, celerity and group velocity are changed as is the wavelength. The changes in wave speed change the direction of wave travel and change the amplitude of the wave, these phenomena are known as refraction and shoaling.

In the expeditive assessment, the precautionary assumption that the direction of wave travel doesn't produce refraction is fixed.

Wave height at the incipient breaking H_b is evaluated by the definition of the breaker indexes.

The breaker depth index is defined as:

$$\gamma_b = \frac{H_b}{d_b}$$

In which d_b is the depth at breaking.

Breaker height index, describing the nondimensional breaker height, is defined as:

$$\Omega_b = \frac{H_b}{H_0}$$

Beaker depth index is evaluated by the expression derived by Weggel (1972)

$$\gamma_b = b - a \frac{H_b}{gT^2}$$

For $\tan\beta \leq 0.1$ and $H'_0 \leq 0.06$, where T is the wave period, g is gravitational acceleration and H'_0 is the equivalent unrefracted deepwater wave depth. The parameters a and b are determined function of beach slope:

$$a = 43.8(1 - e^{-19\tan\beta})$$
$$b = \frac{1.56}{1 + e^{-19.5\tan\beta}}$$

Breaker height index has been estimated by the relation of Komar and Gaughan (1973) derived from linear wave theory

$$\Omega_b = 0.56 \left(\frac{H'_0}{L_0} \right)^{-\frac{1}{5}}$$

Breaker type may be correlated to the surf similarity parameter (or Iribarren number)

$$\xi_0 = \tan \tan \beta \left(\frac{H_0}{L_0} \right)^{-\frac{1}{2}}$$

On uniformly sloping beach, breaker type is estimated by

Surging/collapsing $\xi_0 > 3.3$
 Plunging $0.5 < \xi_0 < 3.3$
 Spilling $\xi_0 < 0.5$

Wave setup is the superelevation of mean water level caused by wave action. Total water depth is a sum of still-water depth and setup

$$d = h + \underline{\eta}$$

Where h is the still-water level and $\underline{\eta}$ is the mean water surface elevation above still-water level.

Lounguet-Higgins and Stewart (1963) obtained setdown for regular waves from the integration of the cross-shore balance of momentum equation governing mean water level, assuming normally incident waves and $\underline{\eta}=0$ in deep water. The maximum lowering of the water level, setdown, occurs near the break point $\underline{\eta}_b$.

$$\underline{\eta} = -\frac{1}{8} \frac{H^2 \frac{2\pi}{L}}{\sinh \sinh \left(\frac{4\pi}{L} d \right)}$$

Setup at the still-water shoreline $\underline{\eta}_s$ is given by

$$\underline{\eta}_s = \underline{\eta}_b + \left[\frac{1}{1 + \frac{8}{3\gamma_b^2}} \right] H_b$$

Runup is the maximum elevation of wave uprush above still-water level. Wave uprush consists in two components: superelevation of the mean water level due to wave action (setup) and fluctuation about that mean (swash).

Irregular wave runup is a function of the surf similarity parameter (CEM 2008, Mase 1989) and is evaluated by the use of the predictive equations. The whole set of runup values is included in the limits defined by the relations below displayed

$$\frac{R_{max}}{H_0} = 2.32 \xi_0^{0.77} \quad \frac{R_{med}}{H_0} = 0.88 \xi_0^{0.69}$$

In which R_{max} is the maximum runup and R_{med} is the mean runup.

It is well known that the coasts of the Mediterranean are characterised by micro-tidal conditions with respect to the Oceans. Therefore, tides are not so relevant for the evaluation of sea storm conditions, which are mainly characterized by wind wave climate both in ordinary and extreme scenarios.

However, for the pilot site a tidal data analysis was performed in terms of harmonic components by acquiring the principal astronomical constituents and assuming a typical annual evolution implemented by available data at 2014.

For the Italian pilot sites, the astronomical constituents, amplitudes and phases have been freely downloaded from The National Tide Gauge Network website (www.mareografico.it) and the signal $F(t)$, in terms of harmonics, has been constructed by super-imposing the individual components. Data are referred to the tidal station named Palermo which can be assumed as representative even for the Ustica site.

Finally, the cumulative effect of SLR and storm surge for different return time and RCP pattern (26, 70 and 85), has been computed along each transect using the value of 3 mt as threshold for storm-surge event.

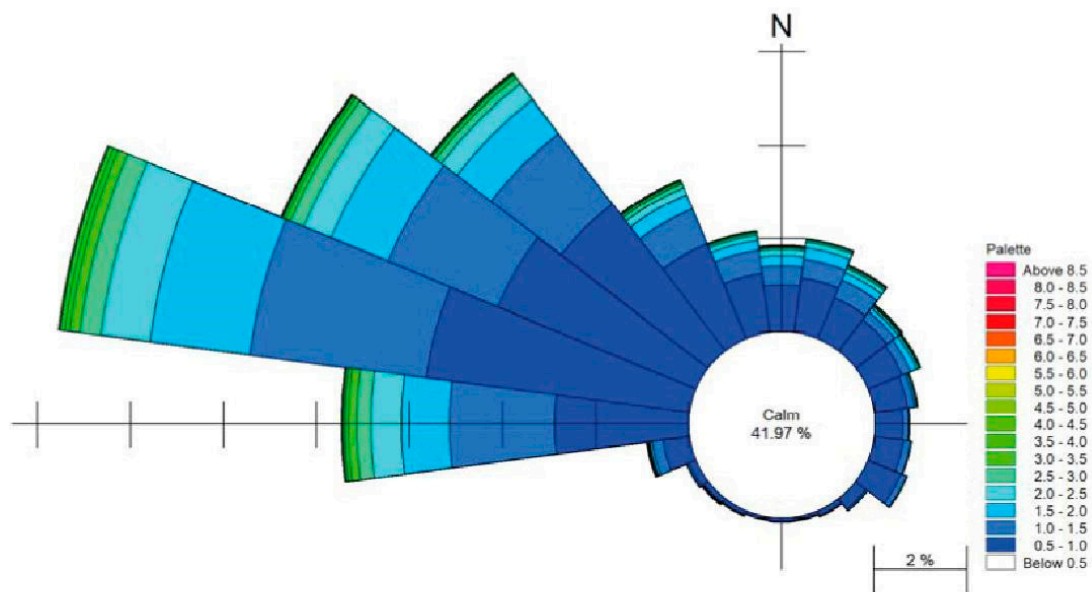


Figure S1 - Prevailing waves directions and heights that strike Ustica Island. The strongest waves come from north-westerly directions, as the prevailing winds are from the NW or W.

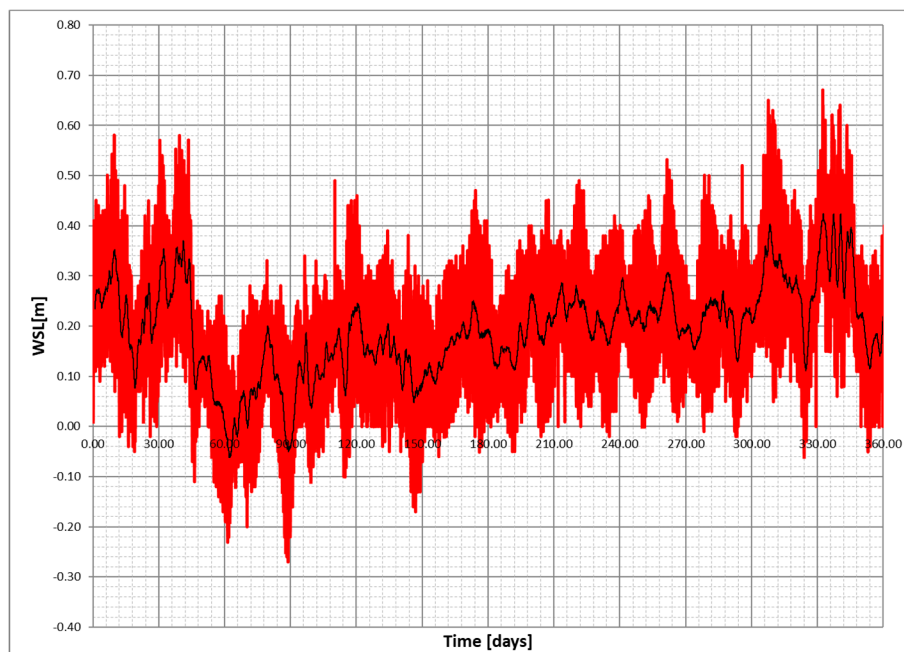


Figure S2SM - Annual harmonic analysis for the tide astronomical constituents. Palermo tide gauge station.

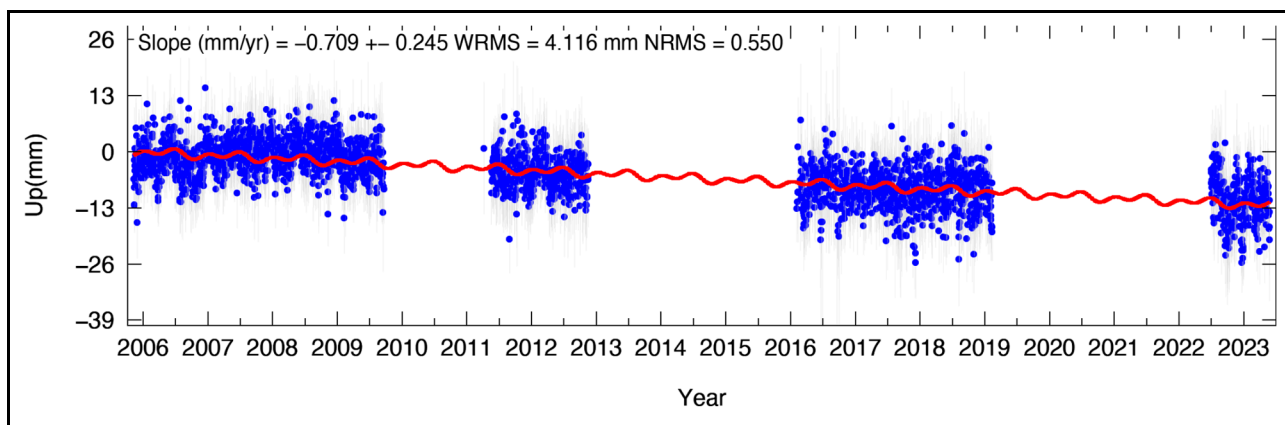
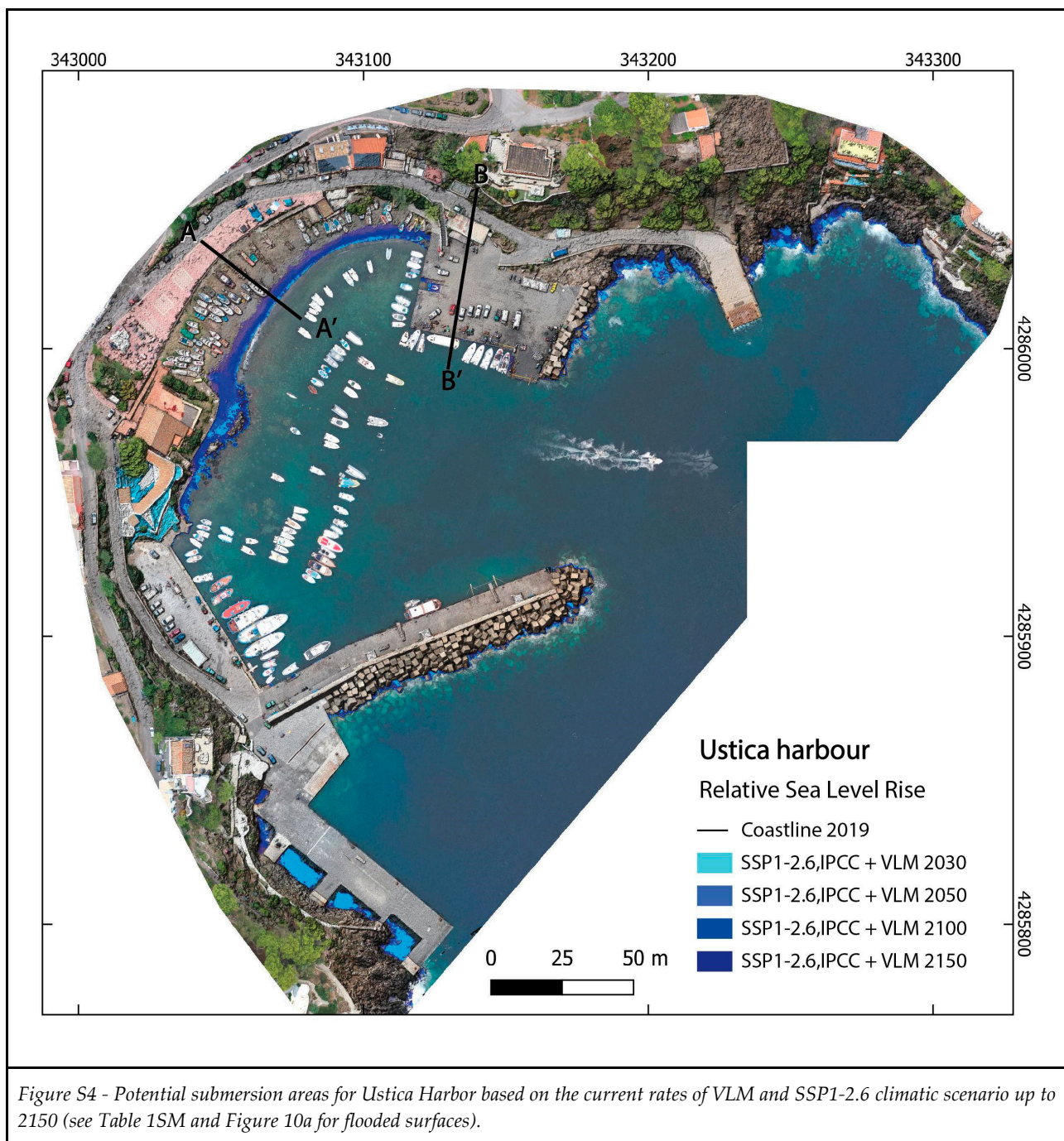
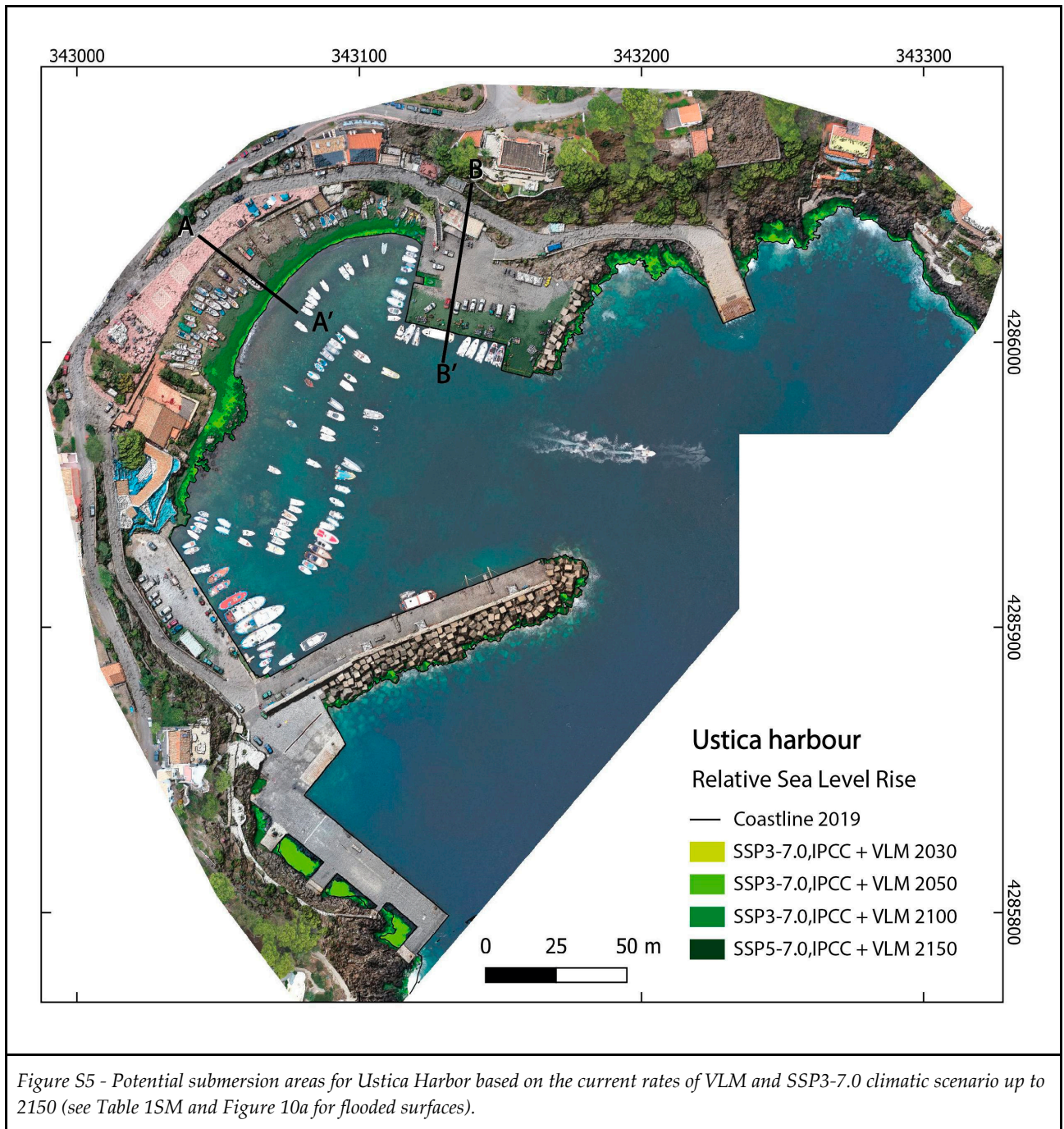


Figure S3 - GPS time series (vertical component) from station UNIX (2006-2023 time interval). In Figure 1b is reported the station location.





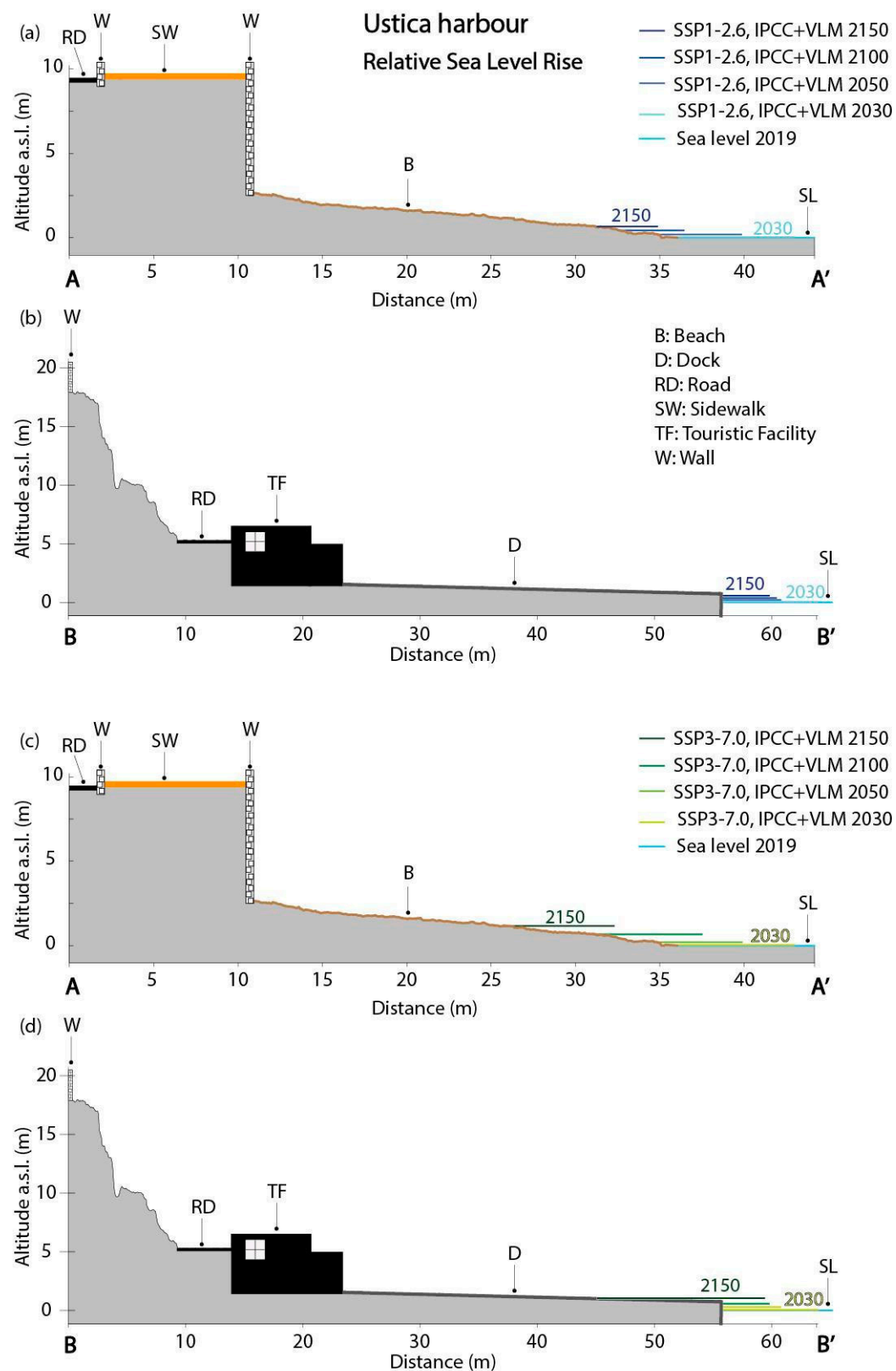


Figure S6 - Cross sections of the expected RSLR for different SSP1 - 2.6 (a and b) and SSP3 - 7.0 (c and d) climatic projections up to 2150 across the beach (AA') and the dock (BB') in the Harbor area. Location of the sections are shown in Figures SM4 and SM5

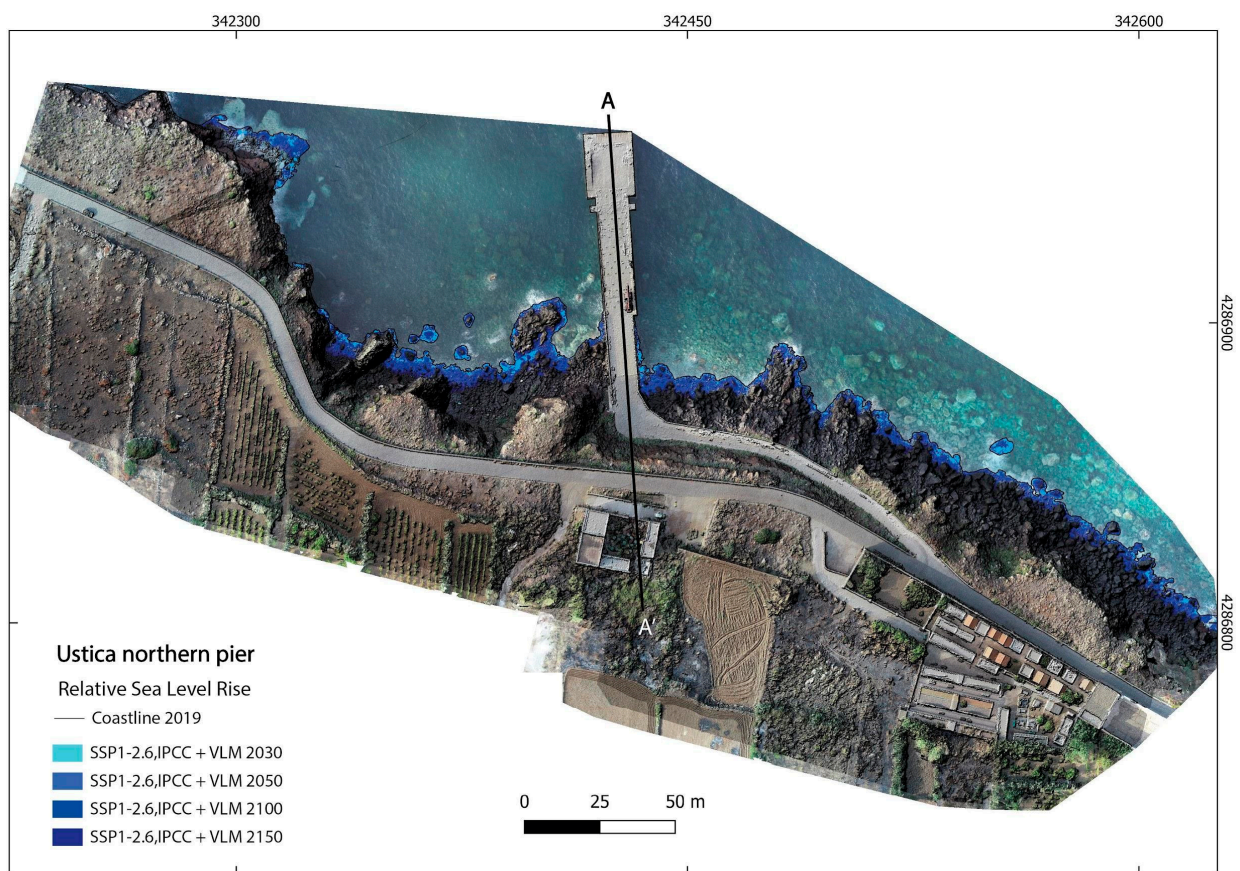


Figure S7 - Potential submersion areas for Ustica Northern Pier (Punta Spalmatore) based on the current rates of VLM and SSP1-2.6 climatic scenario up to 2150 (see Table 1SM and Figure 10c for flooded surfaces).

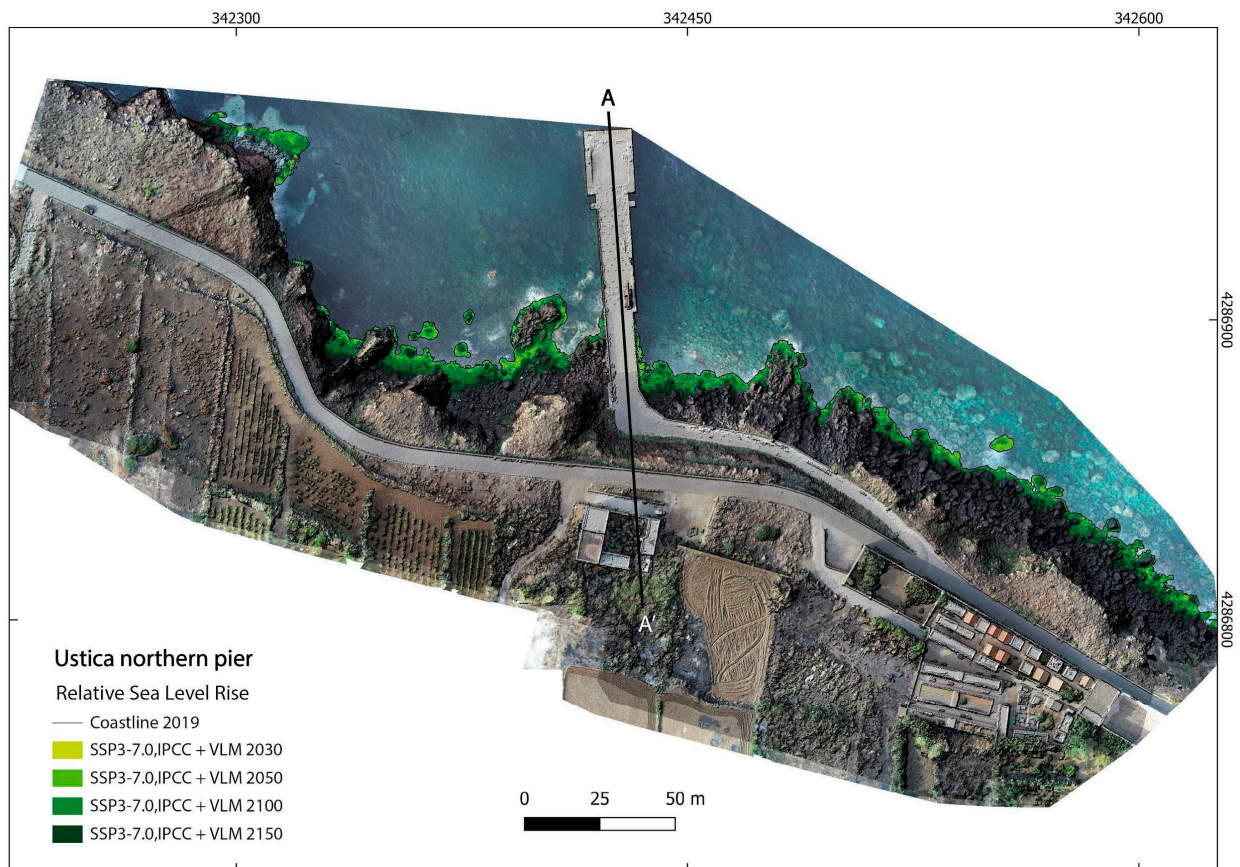


Figure S8 - Potential submersion areas for Ustica Northern Pier (Punta Spalmatore) based on the current rates of VLM and SSP3-7.0 climatic scenario up to 2150 (see Table 1SM and Figure 10c for flooded surfaces).

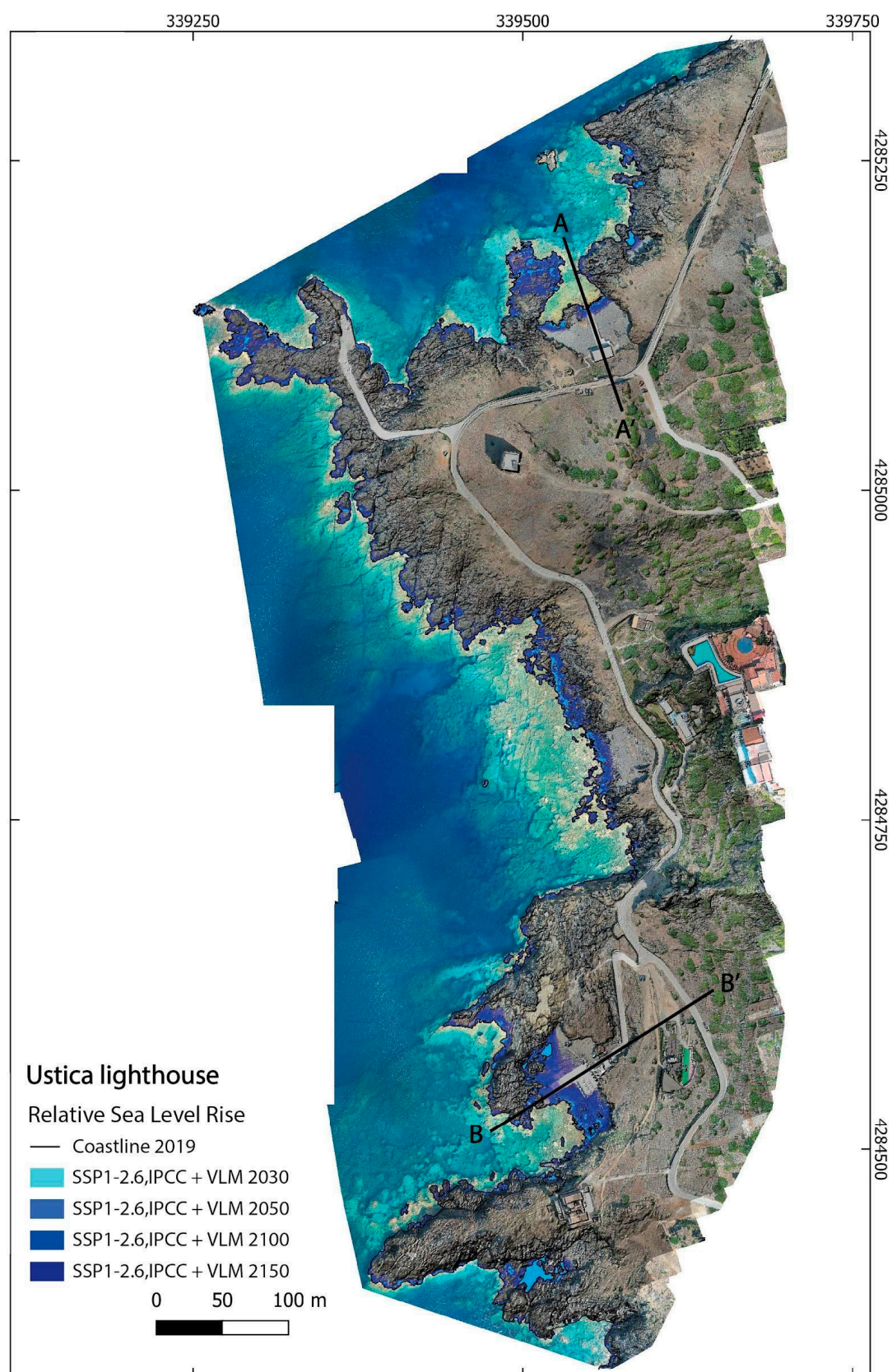


Figure S9 - Potential submersion areas for Ustica Northern Pier (Punta Spalmatore) based on the current rates of VLM and SSP1-2.6 climatic scenario up to 2150 (see Table 1SM and Figure 10b for flooded surfaces).

Ustica lighthouse

Relative Sea Level Rise

- SSP1-2.6, IPCC+VLM 2150
- SSP1-2.6, IPCC+VLM 2030
- SSP1-2.6, IPCC+VLM 2100
- Sea level 2019 (SL)
- SSP1-2.6, IPCC+VLM 2050

P: Parking lot
PV: Pavement
RD: Road
TF: Touristic Facility

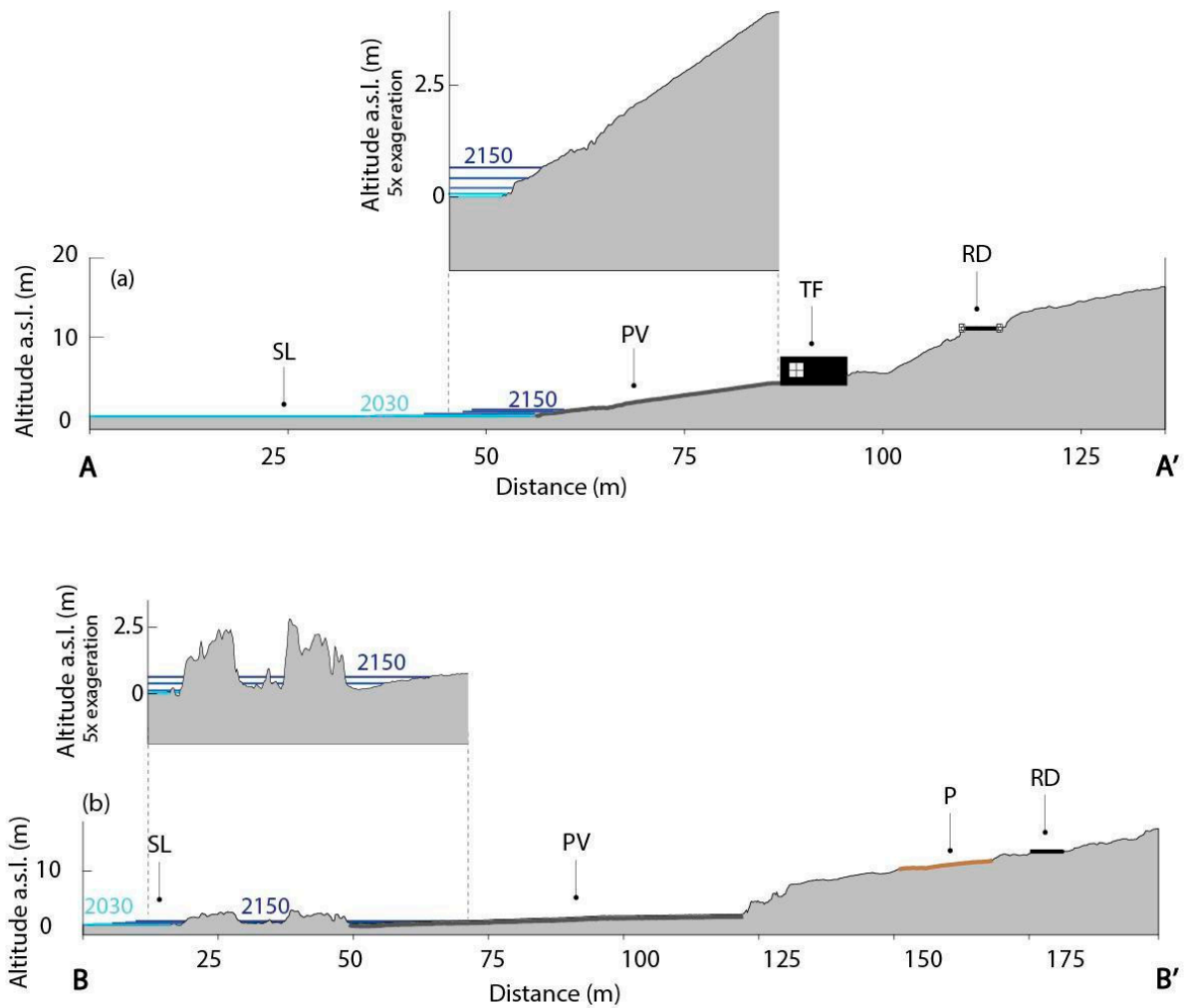


Figure S10 - cross sections of the expected RSLR up to 2150 for SSP1-2.6 climatic projections across the northern (AA') and southern (BB') pocket beaches, as shown in Figure 9SM.

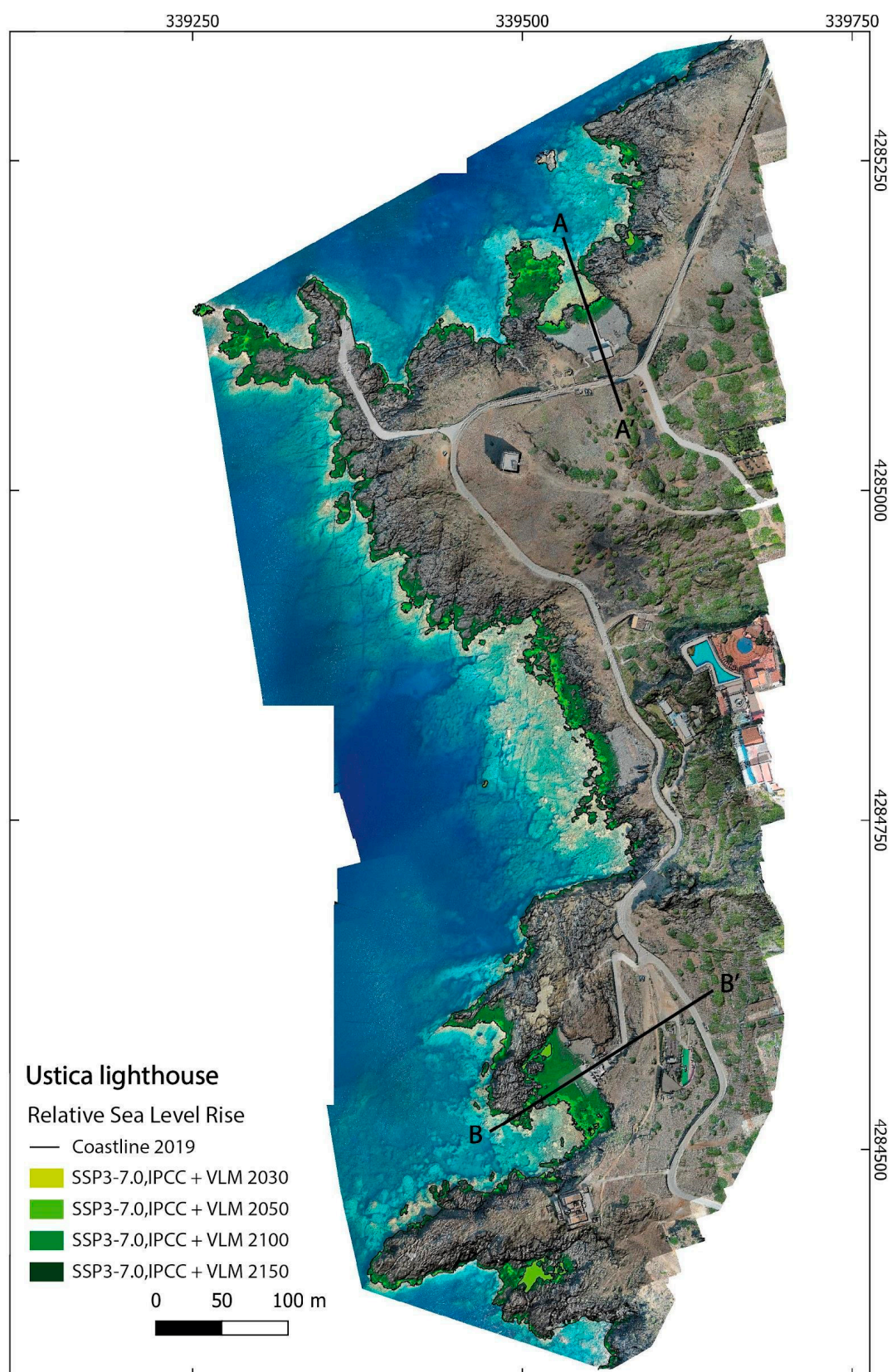


Figure S11 - Potential submersion areas for Ustica Northern Pier (Punta Spalmatore) based on the current rates of VLM and SSP3-7.0 climatic scenario up to 2150 (see Table 1SM and Figure 10b for flooded surfaces).

Ustica lighthouse

Relative Sea Level Rise

- SSP3-7.0, IPCC+VLM 2150
- SSP3-7.0, IPCC+VLM 2030
- SSP3-7.0, IPCC+VLM 2100
- Sea level 2019 (SL)
- SSP3-7.0, IPCC+VLM 2050

P: Parking lot
PV: Pavement
RD: Road
TF: Touristic Facility

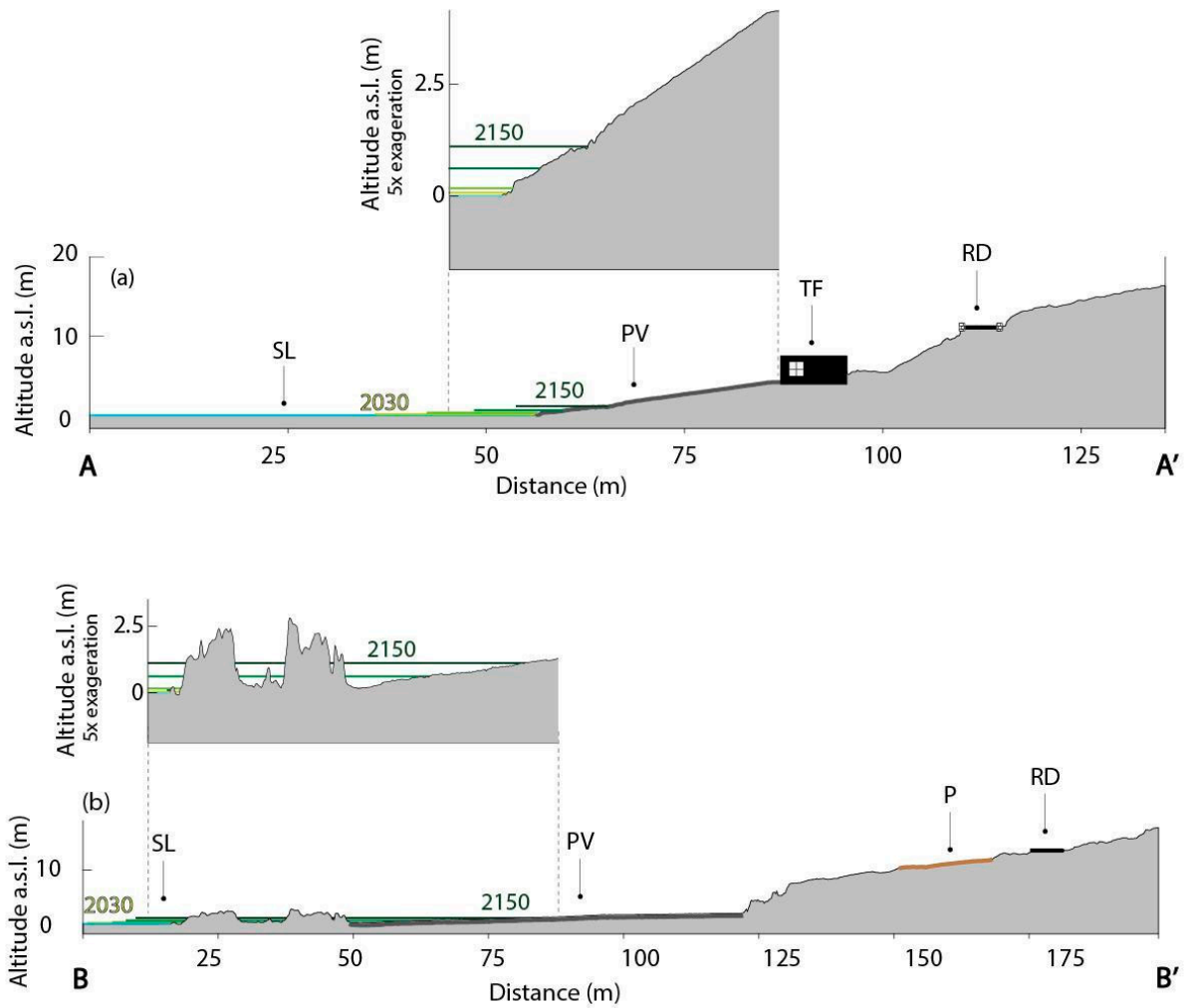


Figure S12 - cross sections of the expected RSLR up to 2150 for SSP3-7.0 climatic projections across the northern (AA') and southern (BB') pocket beaches, as shown in Figure 11SM.

CLIMATIC SCENARIO		RELATIVE SEA LEVEL				FLOODED SURFACE			
SSP Scenario	Year	Ordinary Condition		MaxWL in Storm Surge Condition		Ordinary Condition		MaxWL in Storm Surge Condition	
		SLR + VLM (mm)	σ SLR + VLM (mm)	RT1 (SLR + VLM) (m)	RT100 (SLR + VLM) (m)	SLR + VLM (mq)	SLR + VLM (ha)	RT100 (SLR + VLM) (mq)	RT100 (SLR + VLM) (ha)
Northern Pier									
	2019	0	45	6.5	10.0			7713.1	0.77
SSP1-26	2030	50	68	6.5	10.1	332	0.03		
SSP1-26	2050	159	106	6.6	10.2	532	0.05		
SSP1-26	2100	421	238	6.9	10.4	1148	0.11		
SSP1-26	2150	659	400	7.5	11.1	1534	0.15		
SSP3-70	2030	49	65	6.5	10.2	331	0.03		
SSP3-70	2050	187	109	6.6	10.2	594	0.06		
SSP3-70	2100	643	270	7.1	10.7	1510	0.15		
SSP3-70	2150	1127	484	7.6	11.1	2103	0.21		
SSP5-85	2030	57	62	6.5	10.2	343	0.03	7766.9	0.78
SSP5-85	2050	200	111	6.7	10.2	622	0.06	7766.9	0.78
SSP5-85	2100	741	277	7.2	10.8	1645	0.16	7916.3	0.79
SSP5-85	2150	1278	518	7.7	11.3	2280	0.23	8069.3	0.81
Lighthouse									
	2019	0	45	6.7	10.2			91910.7	9.19
SSP1-26	2030	50	68	6.8	10.2	2369	0.24		
SSP1-26	2050	159	106	6.9	10.3	4267	0.43		
SSP1-26	2100	421	238	7.2	10.6	8679	0.87		
SSP1-26	2150	659	400	7.8	11.2	11931	1.19		
SSP3-70	2030	49	65	6.8	10.3	2286	0.23		
SSP3-70	2050	187	109	6.9	10.3	4746	0.47		
SSP3-70	2100	643	270	7.4	10.8	11717	1.17		
SSP3-70	2150	1127	484	7.9	11.3	17207	1.72		
SSP5-85	2030	57	62	6.8	10.4	2424	0.24	93997.4	9.40
SSP5-85	2050	200	111	6.9	10.4	4954	0.50	93997.4	9.40
SSP5-85	2100	741	277	7.5	10.9	12988	1.30	97819.2	9.78
SSP5-85	2150	1278	518	8.0	11.4	18675	1.87	101549.0	10.15
Harbour									
	2019	0	45	5.4	5.4			14266.5	1.43
SSP1-26	2030	50	68	5.5	5.5	430	0.04		
SSP1-26	2050	159	106	5.6	5.6	645	0.06		
SSP1-26	2100	421	238	5.9	5.9	1251	0.13		
SSP1-26	2150	659	400	6.5	6.5	1717	0.17		
SSP3-70	2030	49	65	5.5	5.6	429	0.04		
SSP3-70	2050	187	109	5.6	5.6	703	0.07		
SSP3-70	2100	643	270	6.1	6.1	1682	0.17		
SSP3-70	2150	1127	484	6.6	6.6	3180	0.32		
SSP5-85	2030	57	62	5.5	5.6	444	0.04	14927.6	1.49
SSP5-85	2050	200	111	5.6	5.6	729	0.07	15086.3	1.51
SSP5-85	2100	741	277	6.2	6.2	1907	0.19	15529.6	1.55
SSP5-85	2150	1278	518	6.7	6.7	3781	0.38	15980.8	1.60

Table S1 - The **Relative sea level** column represents a list of the sea level values in ordinary conditions (or stationary conditions) and during a storm surge having RT = 1 or 100 years, for different climatic scenarios. The **Flooded Surface** column represents a list of the expected area (mq = square metres; ha = hectares) covered by the water in ordinary conditions (or stationary conditions) and during a storm surge having RT = 100 years, for different climatic scenarios. SLR + VLM = Sea Level Rise with the addition of Vertical Land Motion; σ SLR + VLM = standard deviation for Sea Level Rise with the addition of Vertical Land Motion.

Table S2: wave parameters.
H0: significant wave height offshore (which represents the value of the wave relative to a given return time. Data from the Palermo wave buoy);
Tp: peak period of the storm surge waves;
Rmax: maximum "run-up" of the wave as a function of the morphology of the coast;
Tide: tidal surge
MSL: maximum value of sea level rise as the sum of the rise for the reference climatic scenario and storm surges for different return times (1 year and 100 years).
Bottom: the table shows the Sea Level Rise for the SSP3-8.5 scenario (SLR in m) and the relative error (in mm).

1. Komar, P. D., and Gaughan, M. K. (1973), Airy wave theory and breaker height prediction. *Proceedings of the 13th Coastal engineering Conference*, American Society of Civil engineers, pp 405-418
2. Longuet-Higgins, M. S., and Stewart, R. W., (1963). A note on Wave setup, *Journal of Marine Research*, Vol 21, No.1, pp 4-10
3. Mase, H. (1989). Random wave runup height on gentle slope. *Journal of waterway, port, Coastal, and Ocean Engineering*, Vol. 115, No. 5, pp 649-661
4. Mentaschi, L., G. Besio, F. Cassola, and A. Mazzino (2013). Developing and validating a forecast/hindcast system for the Mediterranean sea. *Journal of Coastal Research SI 65*, 1551–1556.
5. Mentaschi, L., G. Besio, F. Cassola, and A. Mazzino (2015). Performance evaluation of WavewatchIII in the Mediterranean Sea. *Ocean Modelling 90*, 82–94.

6. Weggel, J. R. (1972), Maximum breaker height. *Journal of the waterways, harbours and coastal Engineering Division*, Vol 98, No. WW4, pp 529-548